VISIBLE LIGHT SPECTROSCOPIC ANALYSIS OF METHYLENE BLUE IN WATER[**]

A. Fernández-Pérez, G. Marbán*

*Instituto de Ciencia y Tecnología del Carbono (INCAR-CSIC),
33011-Oviedo, Spain; e-mail: greca@incar.csic.es*

We herein report a universal calibration curve for the UV-visible spectrophotometric determination of the concentration of polymerizable dyes in solution. The method has been successfully applied to construct a calibration curve of methylene blue in water that is applicable over a wide range of methylene blue and chloride concentrations, regardless of both the aggregate concentration distribution and the temperature. In addition, it was found that the molar fractions of each methylene blue species in solution could be well approximated by means of simple algebraic expressions in the A_{650}/A_{607} absorbance ratio.

Keywords: *calibration curve, polymerizable dye, methylene blue, UV-visible spectrophotometry, self-aggregation.*

СПЕКТРОСКОПИЧЕСКИЙ АНАЛИЗ ВОДНОГО РАСТВОРА МЕТИЛЕНОВОГО СИНЕГО В ВИДИМОМ ДИАПАЗОНЕ

A. Fernández-Pérez, G. Marbán*

УДК 543.42

*Институт углеродной науки и техники (INCAR-CSIC),
33011 Овьедо, Испания; e-mail: greca@incar.csic.es*

(Поступила 10 ноября 2020)

Получена универсальная калибровочная кривая для определения концентрации полимеризуемых красителей в растворах в УФ-видимом диапазоне методом спектрофотометрии. Метод успешно применен для водных растворов метиленового синего в широком диапазоне концентраций метиленового синего и добавки NaCl независимо от распределения суммарной концентрации и температуры. Показано, что молярные доли каждого вида метиленового синего в растворе могут быть хорошо аппроксимированы с помощью простых алгебраических выражений для соотношения A_{650}/A_{607}.

Ключевые слова: *калибровочная кривая, полимеризуемый краситель, метиленовый синий, УФ-видимая спектрофотометрия, самоагрегация.*

Introduction. The ecotoxicity of dyes in water effluents has attracted widespread interest in the scientific community during recent years and motivated the development of a number of water treatment methods to remove these contaminants, with adsorption, photocatalysis, and biodegradation the main processes studied [1, 2]. In those studies, the colored nature of dyes meant that spectrometry in the UV-Vis range became the most often used analysis tool. For the evaluation of the concentration of an unknown sample, a calibration curve must be constructed beforehand. A calibration curve is created by first preparing a set of standard solutions with known concentrations of the analyte. The instrument response is measured for each and plotted against the concentration of the standard solution. Common practice for producing the calibration curve with a UV-Vis spectrophotometer is based on the linear relationship between the absorbance and the dye concentration at a given wavelength, according to the Beer-Lambert law:

$$C_{\text{dye}} = \beta A_\lambda / I_F L, \quad (1)$$

[**]Full text is published in JAS V. 88, No. 6 (http://springer.com/journal/10812) and in electronic version of ZhPS V. 88, No. 6 (http://www.elibrary.ru/title_about.asp?id=7318; sales@elibrary.ru).

where C_{dye} is the dye concentration (mol/L), A_λ is the absorbance at the λ wavelength, β is the inverse of ε_λ, the molar attenuation coefficient of the solution at the same wavelength (L/mol · cm), L is the path length (cm) and I_F is an instrumental factor that ensures that the molar attenuation factors evaluated with a given solution are independent of the cuvette used for the evaluation [3]. Ideally, the values of I_F should be 1 when the cuvettes materials show exactly the same transmittance for each cuvette and the true path lengths are equal to the nominal path lengths (L). To build the calibration curve of aqueous solutions of methylene blue (MB), the wavelength at the maximum absorbance (~664 nm) is typically used. However, deviations from linearity in the relationship between A_{664} and C_{MB} are commonplace [4–10]. These deviations must be ascribed to the tendency of the dyes in solution to aggregate, affecting the shape of the UV-Vis spectra. In the case of methylene blue, the long scientific effort to provide reliable identification of aggregates existing in solution together with accurate optical and thermodynamic parameters of formation of the different species [11—30] has recently been successful [3]. In aqueous MB solutions, monomer molecules, dimers and tetramers coexist in a wide range of MB and chloride concentrations [3], exhibiting quite different absorption spectra (Fig. 1) [3, 31]. The Supplementary Information file includes a short summary of the methods used to prove the presence of each species.

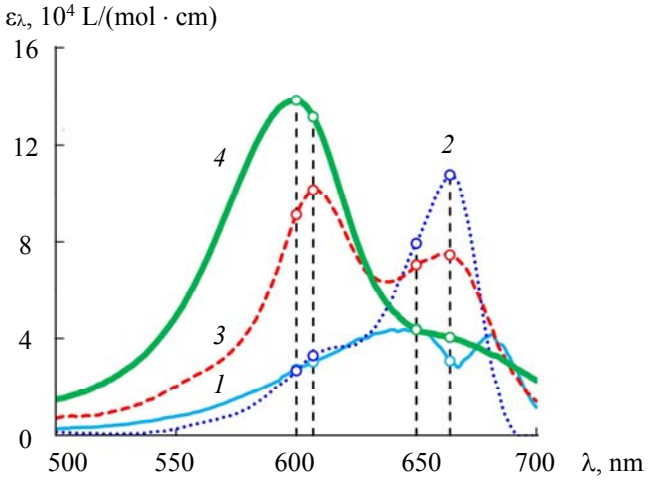

Fig. 1. Optical spectra for all the MB species either virtually (mesomers) or truly contained in aqueous solutions, 1 – monomer (mesomer I), 2 – monomer (mesomer II), 3 – dimer, 4 – tetramer.

We have proven that the monomer exhibits a temperature-dependent absorption behaviour that is caused by the change in its electron charge distribution with the variation in the temperature-dependent dielectric constant of water. The monomer charge distribution lies between those of two virtual resonance forms, with the absorption spectrum of the monomer being a composition of the theoretical spectra for the virtual mesomers (Fig. 1), the proportions of which are established by a temperature-dependent virtual equilibrium constant (resonance virtual equilibrium hypothesis) [31].

The molar fractions of the monomeric, dimeric, and tetrameric forms are highly dependent on both the total concentration of MB molecules and the temperature. Surprisingly, to the best of our knowledge, is the fact that the obvious distortion introduced into the shape of the standard calibration curve (Eq. (1)) by the self-aggregation phenomenon has never been considered. The taken-for-granted use of the standard calibration curve at the maximum wavelength in all modern studies [32–41] is concrete evidence of that. This approximation may be valid for small concentration ranges, though the application conditions should be the result of a complex decision-making process to tackle the measurement uncertainty [4, 42]. The present study is the final piece of a detailed research project into the self-aggregation behaviour of methylene blue in water [3, 31]. Here, we describe a simple way to build the calibration curve of aqueous methylene blue and, by extension, of any polymerizable dye in water. The calibration curve can be applied to a wide range of MB and chloride concentrations regardless of both the aggregate concentration distribution and the temperature, and thus merits the label universal.

Experimental. The absorption spectra (400–800 nm) of 56 aqueous MB solutions in the 1.1×10^{-6}–3.4×10^{-3} mol/L concentration range, in which different NaCl amounts were added (0.00–0.15 mol/L), were obtained at four different temperatures in the 282–333 K range using a UV-Visible spectrometer (Shimadzu UV-2401PC), giving a total of 224 spectra. The temperature of the optical cuvettes was kept constant using a Lauda Alpha RA8 thermo circulating bath. Every measurement was performed in triplicate, with exhaustive cleaning of the cuvettes (water, ethanol, and air drying) between measurements. A total of three optical cuvettes were used for all the analyses (two cuvettes of 1 cm and one cuvette of 0.01 cm). The instrumental factors were evaluated for all cuvettes [I_F = 1, 1.004 (1 cm path length) and 1.145 (0.01 cm path length)].

The universal calibration curves. The method consists of simply using the Beer-Lambert equation at each of the wavelengths of the absorbance spectrum that are characteristic of the optical spectra of the different species in solution, either monomeric or aggregates. We consider the characteristic wavelengths to be those corresponding to the absorption maxima (empty circles in Fig. 1). The characteristic wavelengths and corresponding values of molar attenuation coefficients of the different MB species are listed in Table 1. Thus, application of the Beer–Lambert equation to the absorption spectrum of a polymerizable dye yields:

$$A_{\lambda_i} = \sum_{j=1}^{m} A_{\lambda_i j} = I_F L \sum_{j=1}^{m} \left(\varepsilon_{\lambda_i j} C_j \right), \tag{2}$$

where i is the summation index from 1 to m wavelengths (in the case of MB, $m = 4$ and $\lambda_1 = 650$ nm, $\lambda_2 = 664$ nm, $\lambda_3 = 607$ nm, and $\lambda_4 = 600$ nm) and j is the summation index from 1 to m species (in the case of MB, mesomer I when $j = 1$, mesomer II when $j = 2$, trimer when $j = 3$, and tetramer when $j = 4$) [3, 31]. The molar attenuation coefficients $\varepsilon_{\lambda_i j}$ of the different MB species are shown in Table 1. The dye species concentrations C_j are the m unknowns in the system of Eq. (2). The total dye concentration can be evaluated by the mass balance as

$$C_{dye} = \sum_{j=1}^{m} n_j C_j, \tag{3}$$

where n_j is the aggregation order, which is to say the number of single dye molecules of each species (in the case of MB, $n_1 = 1$, $n_2 = 1$, $n_3 = 2$, and $n_4 = 4$ for mesomer I, mesomer II, dimer, and tetramer, respectively). By solving the system of Eq. (2) with Cramer's rule and entering the result in Eq. (3), the following equation is obtained:

$$C_{dye} = \frac{1}{I_F L} \sum_{i=1}^{m} \left(\beta_i A_{\lambda_i} \right) \tag{4}$$

in which

$$\beta_i = \frac{\sum_{j=1}^{m} \left[(-1)^{i+j} n_j \alpha_{\lambda_i j} \right]}{\begin{bmatrix} \varepsilon_{\lambda_1 1} & \cdots & \varepsilon_{\lambda_1 m} \\ \vdots & \ddots & \vdots \\ \varepsilon_{\lambda_m 1} & \cdots & \varepsilon_{\lambda_m m} \end{bmatrix}}, \tag{5}$$

where $\alpha_{\lambda_i j}$ is the (i, j) minor of the $m\times m$ matrix formed by the $\varepsilon_{\lambda_i j}$ coefficients, whose determinant is the denominator of Eq. (5). Thus, the β_i proportionality coefficients only depend on the values of the molar attenuation coefficients and the aggregation order (n_j values) and are independent of other variables such as temperature, degree of aggregation, or ionic strength. Therefore, if the optical spectra of the different monomers and aggregates are known, Eq. (4) should be applicable as a universal calibration curve for any polymerizable dye. Such is the case of MB, whose β_i parameters evaluated as explained above are indicated in Table 1.

Figure 2 shows the normalized absorbance spectra of the MB solutions analysed at 282 K. An equal number of spectra, not included here, were measured at each of the other three temperatures (296, 313, and 333 K), with curve shape trends being similar to those observed in Fig. 2.

TABLE 1. Molar Attenuation Coefficients of the Different MB Species [3, 31]

λ_i, nm	Mesomer I $\varepsilon_{\lambda_i 1}$, L/mol cm	Mesomer II $\varepsilon_{\lambda_i 2}$, L/mol cm	Dimer $\varepsilon_{\lambda_i 3}$, L/mol cm	Tetramer $\varepsilon_{\lambda_i 4}$, L/mol cm	β_i, $\times 10^5$
650	43988.4	79417.0	70522.3	43759.4	1.8830
664	30853.3	107751.5	74672.5	40573.3	–0.5213
607	30401.1	33020.1	101444.8	131649.4	–7.9365
600	27479.3	26894.8	91212.0	138491.0	9.9905

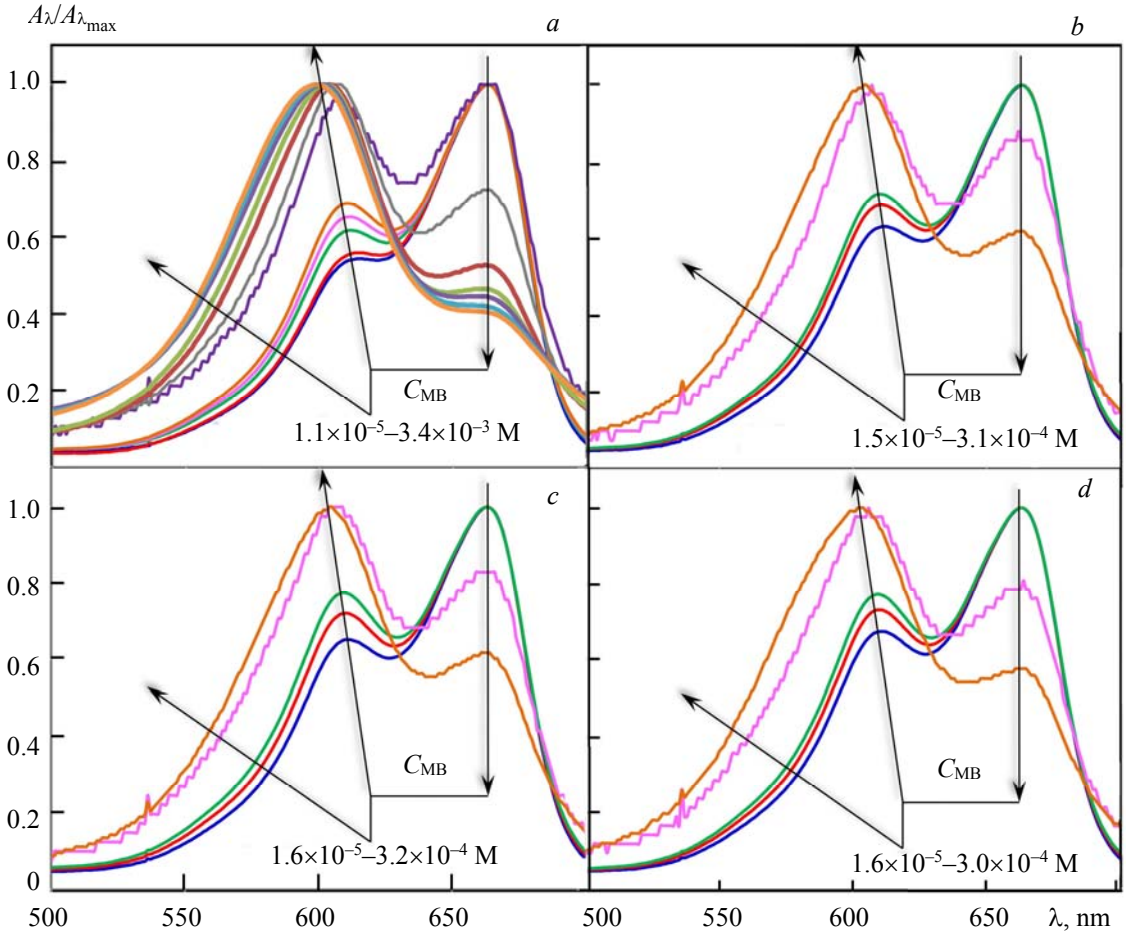

Fig. 2. Normalized absorbance (absorbance divided by maximum absorbance) spectra at 282 K, C_{NaCl} = 0 (a), 0.5 (b), 0.10 (c), and 0.15 M (d).

The blueshift on increasing the MB and chloride concentrations is evident, which means that the MB concentration can in no way be predicted with confidence by means of the standard calibration curve (Eq. (1)) over the full concentration and temperature ranges used in the measurements (Fig. 3). In fact, the standard deviation of the mean relative error in C_{MB}, used as an error function in the optimization of β in Eq. (1) with the 224 experimental points ($\beta = 2.04\times10^{-5}$), is as high as 37.2%. With Eq. (1), the C_{MB} values are clearly overestimated at low MB concentrations and underestimated at high concentrations, exhibiting a great dispersion for a given value of C_{MB} due to differences in temperature and/or chloride concentration (Fig. 3). On the other hand, Eq. (4) demonstrates a more than satisfactory prediction (Fig. 3) with a mean relative error as low as 0.00 ± 3.16%. This error was obtained via an error minimization procedure in which the I_F values were optimized with respect to those evaluated experimentally, though the differences between

experimental and optimized values were found to be negligible (1 versus 1, 1.004 versus 1.018 and 1.145 versus 1.153 for the experimental and optimized values of the three cuvettes, respectively).

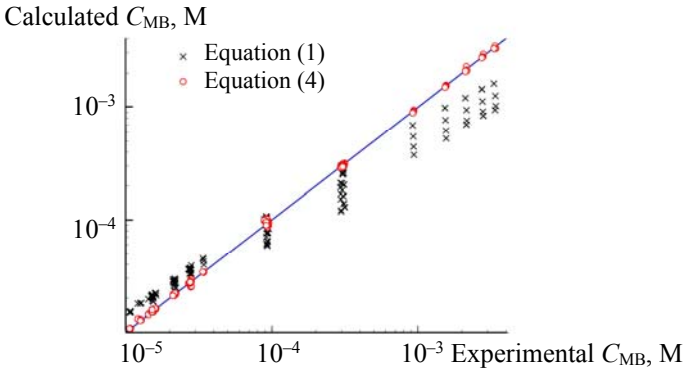

Fig. 3. Comparison between the standard (crosses) and universal (circles) calibration curves.

In addition to the characteristic wavelengths, Eq. (4) was tested with all wavelengths in the 500–700 nm range though no improvement in the calibration error was seen. When the molar attenuation coefficients of the different species in solution for a given dye are unknown, the universal calibration curve might still be used if a given value of m is assumed and the characteristic wavelengths of each of the m species can be approximated by a rational approach. In such a case, the β_i values can be obtained by error minimization. In fact, even when the attenuation coefficients are known, as in the case of MB, small differences in instrument sensitivity might cause the β_i coefficients listed in Table 1 to work slightly incorrectly with absorbance spectra of MB solutions produced by a different analyser to the one used in this study, in which case the proper procedure is to again optimize the β_i coefficients via error minimization, this time using the absorbance values at the same wavelengths as those indicated in Table 1 and the values of β_i shown in the same table as initial estimates.

For predictive purposes, it would be interesting to find an easy way to relate the molar fraction of each species in solution ($X_j = n_j C_j / C_{dye}$) to the values of absorbance at their characteristic wavelengths. The following expression is obtained from Eqs. (2) and (3):

$$X_j = \frac{n_j \sum_{i=1}^{m} \left[(-1)^{i+j} \alpha_{\lambda_i j} A_{\lambda_i} \right]}{\sum_{i=1}^{m} \left\{ \left[\sum_{j=1}^{m} \left((-1)^{i+j} n_j \alpha_{\lambda_i j} \right) \right] A_{\lambda_i} \right\}}. \quad (6)$$

However, this expression is complex and can result in a significant error with even a very small difference in instrument sensitivity. From a practical point of view, the most important thing is to relate each fraction to the ratio of a single pair of characteristic absorbances so that we may have an easy and sufficiently accurate evaluation of the molar fractions with just two points on the absorbance spectra, regardless of type of cell, dye concentration, ionic strength or temperature. Of course, this procedure cannot yield the same

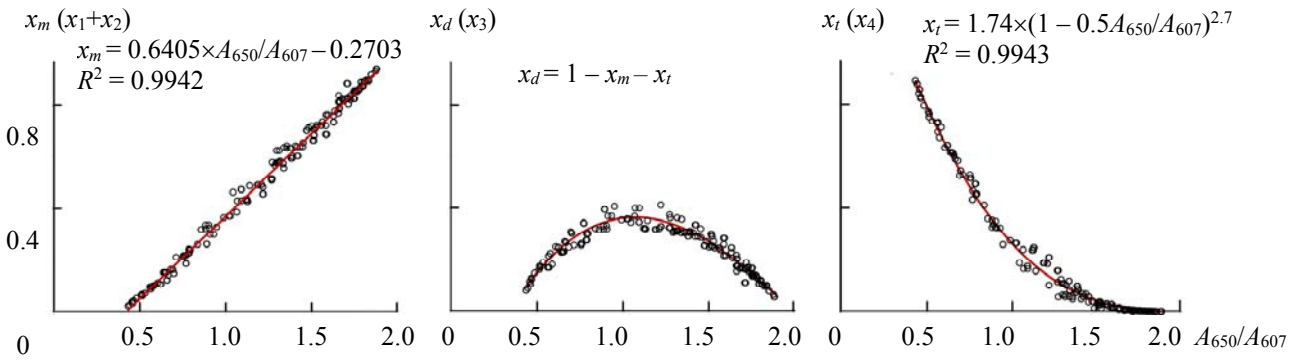

Fig. 4. Variation of the molar fraction of the different MB species in solution with the A_{650}/A_{607} ratio.

result for the whole set of conditions at a given absorbance ratio, since the molar fractions depend on the characteristic absorbances for all species (Eq. (6)). It may, however, yield a fair approximation. In this study we evaluated the molar fractions of the different MB species for all solutions prepared in the study by following the methodology described in our previous work [3]. Then we plotted these values against the different $A_{\lambda i}/A_{\lambda k}$ ratios ($1 \le i, k \le 4$, $i \ne k$) and found that the best correlations were when using the A_{650}/A_{607} ratio. Figure 4 shows these correlations for the monomer (X_m), dimer (X_d) and tetramer (X_t). The algebraic expressions that relate the different molar fractions to the A_{650}/A_{607} ratio are indicated in the figure. The regression coefficients are over 0.99 in all cases. Considering that the points displayed in Fig. 4 cover wide ranges of MB concentrations ($1.1\times10^{-6} \le C_{MB} \le 3.4\times10^{-3}$ mol/L), ionic strengths ($1.1\times10^{-6} \le [Cl^-] \le 0.15$ mol/L) and temperatures (282–333 K), the values evaluated with the algebraic expressions can be regarded as sufficiently precise.

Conclusions. A universal calibration curve for the UV-Vis spectrophotometric determination of the concentration of polymerizable dyes in solution was deduced from the Beer–Lambert law. The dye concentration is a linear function of the absorbance values at the characteristic wavelengths. The proportionality coefficients only depend on the values of the molar attenuation coefficients and the aggregation order and are independent of other variables such as temperature, degree of aggregation, or ionic strength. These coefficients can be evaluated either with the molar attenuation coefficients of the different dye species (if known) or via error minimization. The method has been successfully applied to construct a calibration curve for methylene blue in water over a wide range of methylene blue and chloride concentrations, regardless of both the aggregate concentration distribution and the temperature. The molar fractions of each MB species in solution were well approximated by means of simple algebraic expressions in the A_{650}/A_{607} absorbance ratio.

Acknowledgements. The financial support for this research work provided by the Spanish MINECO (CTM2014-56770-R project) and FEDER Funds (GRUPIN2018 (IDI/2018/000148), Principado de Asturias) is gratefully acknowledged. AFP is grateful to the Spanish MINECO for the award of a contract (BES-2015-072274).

REFERENCES

1. R. Croce, F. Cinà, A. Lombardo, G. Crispeyn, C. I. Cappelli, M. Vian, et al., *Ecotoxicol. Environ. Saf.,* **144**, 79–87 (2017), doi: 10.1016/j.ecoenv.2017.05.046.
2. E. Forgacs, T. Cserháti, G. Oros, *Environ. Int.*, **30**, No. 7, 953–971 (2004), doi: 10.1016/j.envint.2004.02.001.
3. A. Fernández-Pérez, G. Marbán, *ACS Omega*, **5**, N 46, 29801–29815 (2020), acsomega.0c03830.
4. N. F. Rosa, O. C. Monteiro, M. F. Camões, R. J. N. B. da Silva, *Acc.. Qual. Assur.*, **22**, No. 4, 217–226 (2017), doi: 10.1007/s00769-017-1272-x.
5. G. Marbán, T. T. Vu, T. Valdés-Solís, *Appl. Catal. A Gen.*, **402**, 1–2 (2011), doi: 10.1016/j.apcata.2011.06.009.
6. R. Nosrati, A. Olad, S. Shakoori, *Mater. Sci. Eng. C*, **80**, 642–651 (2017), doi: 10.1016/j.msec.2017.07.004.
7. H. Masoumbeigi, A. Rezaee, *Heal. Policy Sustain. Heal.*, **2**, 160–166 (2015).
8. A. B. Saleh, M. Abudabbus, *World Acad. Sci. Eng. Technol. Int. Sch. Sci. Res. Innov.*, **7**, 6–22 (2013).
9. D. Malik, C. Jain, A. Yadav, R. Kothari, V. Pathak, IRJET, **3**, No. 7, 864–880 (2016).
10. M. Hossain, M. Ali, T. Islam, *Int. Lett. Chem. Phys. Astron.*, **77**, 26–34 (2018), doi: 10.18052/www.scipress.com/ILCPA.77.26.
11. E. Rabinowitch, L. F. Epstein., *J. Am. Chem. Soc.*, **63**, No. 1, 69–78 (1941), doi: 10.1021/ja01846a011.
12. G. N. Lewis, O. Goldschmid, T. T. Magel, J. Bigeleisen, *J. Am. Chem. Soc.*, **65**, No. 6, 1150–1154 (1943), doi: 10.1021/ja01246a037.
13. D. R. Lemin, T. Vickerstaff, *Trans. Faraday Soc.*, **43**, 491–502 (1947), doi: 10.1039/TF9474300491.
14. K. Ghosh Ashish, *Z. Phys. Chem.*, **94**, No. 4-6, 161 (1975), doi: 10.1524/zpch.1975.94.4-6.161.
15. K. Bergmann, C. T. O'Konski, *J. Phys. Chem. Am. Chem. Soc.*, **67**, No. 10, 2169–2177 (1963), doi: 10.1021/j100804a048.
16. H. Dunken, D. Schmidt, K. Palm, *Z. Chem.*, **2**, No. 11, 349 (1962), doi: 10.1002/zfch.19620021121.
17. W. Spencer, J. R. Sutter, *J. Phys. Chem. Am. Chem. Soc.*, **83**, No. 12, 1573–1576 (1979), doi: 10.1021/j100475a004.

18. O. Yazdani, M. Irandoust, J. B. Ghasemi, S. Hooshmand, *Dye Pigment*, **92**, No. 3, 1031–1041 (2012), doi: 10.1016/j.dyepig.2011.07.006.
19. J. B. Ghasemi, M. Miladi, *J. Chinese Chem.*, **56**, No. 3, 459–468 (2009), doi: 10.1002/jccs.200900069.
20. P. J. Hillson, R. B. McKay, *Trans. Faraday Soc,*, **61**, 374–382 (1965), doi: 10.1039/TF9656100374.
21. K. Patil, R. Pawar, P. Talap, *Phys. Chem. Chem. Phys.*, **2**, No. 19, 4313–4317 (2000).
22. D. Heger, J. Jirkovsk, P. Kln, *J. Phys. Chem.*, **109**, No. 30, 6702–6709 (2005), doi: 10.1021/jp050439j.
23. E. Braswell, *J. Phys. Chem. Am. Chem. Soc.*, **72**, No. 7, 2477–2483 (1968), doi: 10.1021/j100853a035.
24. Z. Zhao, E. R. Malinowski, *Appl. Spectrosc.*, **53**, No. 12, 1567–1574 (1999), doi: 10.1366/0003702991946028.
25. G. Scheibe, *Kolloid-Zeitschrift.*, **82**, No. 1, 1–14 (1938), doi: 10.1007/BF01509409.
26. A. K. Ghosh, P. Mukerjee, *J. Am. Chem. Soc*., **92**, No. 22, 6408–6412 (1970), doi: 10.1021/ja00725a003.
27. Z. Klika, P. Čapková, P. Horáková, M. Valášková, P. Malý, R. Macháň, et al., *J. Colloid Interface Sci.*, **311**, No. 1, 14–23 (2007), doi: 10.1016/j.jcis.2007.02.034.
28. Z. Klika, *Sborník Vědeckých Pr. VŠB-TUOstrava*, **2**, 53 (1979).
29. Z. Zhao, E. R. Malinowski, *J. Chemom*., **13**, No. 2, 83–94 (1999), doi: 10.1002/(SICI)1099-128X(199903/04)13:2<83::AID-CEM529>3.0.CO;2-2.
30. B. Hemmateenejad, G. Absalan, M. Hasanpour, *J. Iran. Chem. Soc*., **8**, No. 1, 166–175 (2011), doi: 10.1007/bf03246213.
31. A. Fernández-Pérez, T. Valdés-Solís, G. Marbán, *Dye Pigment*, **161**, 448–456 (2019).
32. X. Yang, W. Chen, J. Huang, Y. Zhou, Y. Zhu, C. Li, *Sci. Rep*., **5** (2015).
33. G. M. R. Kpinsoton, H. Karoui, Y. Richardson, B. N. S. Koffi, H. Yacouba, J. Motuzas, et al., *React. Kinet. Mech. Catal*. (**2018**), doi: 10.1007/s11144-018-1406-0.
34. L. Wolski, M. Ziolek, *Appl. Catal. B Environ*., **224**, 634–647 (2018), doi: 10.1016/j.apcatb.2017.11.008.
35. A. Houas, H. Lachheb, M. Ksibi, E. Elaloui, C. Guillard, J.-M. M. Herrmann, *Appl. Catal. B Environ.*, **31**, No. 2, 145–157 (2001), doi: 10.1016/S0926-3373(00)00276-9.
36. H. Lachheb, E. Puzenat, A. Houas, M. Ksibi, E. Elaloui, C. Guillard, et al., *Appl. Catal. B Environ.*, **39**, No. 1, 75–90 (2002), doi: 10.1016/S0926-3373(02)00078-4.
37. R. S. Dariani, A. Esmaeili, A. Mortezaali, S. Dehghanpour, *Optik (Stuttg)*, **127**, No. 18, 7143–7154 (2016), doi: 10.1016/j.ijleo.2016.04.026.
38. C. Yogi, K. Kojima, N. Wada, H. Tokumoto, T. Takai, T. Mizoguchi, et al., *Thin Solid Films*, **516**, No. 17, 5881–5884 (2008), doi: 10.1016/j.tsf.2007.10.050.
39. J. H. Potgieter, *J. Chem. Educ.*, **68**, No. 4, 349 (1991), doi: 10.1021/ed068p349.
40. M. R. Bayati, F. Golestani-Fard, A. Z. Moshfegh, *Appl. Catal. A Gen*., **382**, No. 2, 322–331 (2010), doi: 10.1016/j.apcata.2010.05.017.
41. N. Soltani, E. Saion, W. Mahmood Mat Yunus, M. Navasery, G. Bahmanrokh, M. Erfani, et al., *Sol. Energy*, **97**, 147–154 (2013), doi: 10.1016/j.solener.2013.08.023.
42. R. J. N. Bettencourt da Silva, *Talanta*, **148**, 177–190 (2016), doi: 10.1016/j.talanta.2015.10.072.